3Pa2-5

Proceedings of Symposium on Ultrasonic Electronics, Vol. 33 (2012) pp. 327-328
13-15 November, 2012

# Improvement of Selectivity of Closed Cracks in Nonlinear Ultrasonic Imaging by Using Amplitude Difference of Fundamental Wave

## 基本波の振幅差分を用いた非線形超音波映像法による閉口き裂の選択性向上

Masako Ikeuchi[1†], Kentaro Jinno[1], Yoshikazu Ohara[1] and Kazushi Yamanaka[1]
([1]Grad. School Eng., Tohoku Univ.)
池内雅子 [1†]，神納健太郎 [1]，小原良和 [1]，山中一司 [1]([1] 東北大院 工)

## 1. Introduction

We have focused on the subharmonic wave[1)] generated at closed cracks, and have developed a practical closed-crack imaging apparatus, subharmonic phased array for crack evaluation (SPACE).[2)] However, linear scatterers such as back surfaces appeared as ghosts due to filtering leakage in subharmonic array (SA) image, degrading the selectivity of closed cracks. In medical ultrasonics, the selectivity enhancemnt of nonlinear scatterers such as bubbles has been proposed by subtracting a nonlinear image at a small input multiplied by an amplification factor from that at a large input, after creating two nonlinear images by filtering received waves at nonlinear component.[3)] In solid, a similar method, scaling subtraction method (SSM)[4)] was proposed although it claims an advantage of using unfiltered waveforms. We proposed the amplitude difference (AD) method similar to Ref. 3) based on the SPACE, and demonstrated the improvement of the selectivity of closed cracks with the damped double nodes (DDNs) simulation[5)] and an experiment.[6)] However, it could not completely eliminate the ghosts of back surface because the subharmonic waves generated at closed crack are reflected from the back surface and return to the transducer.[6)]

On the other hand, it is reported that not only superharmonic and subharmonic waves but also fundamental wave is generated at closed cracks, exhibiting the threshold phenomena.[7)] In this study, we propose a novel method to dramatically enhance the selectivity of closed cracks based on this phenomenon, and verify its advantage over the AD of subharmonic waves.[6)]

## 2. AD method of fundamental waves

Figure 1 shows the principle of improving the selectivity of closed cracks which utilizes the nonlinearity of the crack responses in the fundamental array (FA) images at different input amplitudes. In the FA image [Fig. 1(b)] at a small input amplitude $u_0$, the closed crack C is not imaged and only the back surfaces S1 and S2 are imaged since the ultrasound is transmitted at the closed crack. However, in the FA image [Fig. 1(a)] at a large input amplitude $au_0$, C is imaged since not only superharmonic and subharmonic waves but also fundamental waves are generated[7)] by the contact vibration of closed cracks. On the other hand, amplitude of S2 is decreased when the transmission is not complete. Therefore, by subtracting the FA image [Fig. 1(b)] multiplied by the amplification factor $a$ from the FA image [Fig. 1(a)], C appears as increment. On the other hand, S1 and S2 appear as 0 and decrement, respectively. Thus, in the subtracted image [Fig. 1(c)] showing only the increment, only C can be imaged with canceling S. Furthermore, spatial resolution can be enhanced since a fundamental wave has twice the frequency of a subharmonic wave. Thus, the AD method of fundamental waves realizes an imaging of closed cracks with high selectivity and high spatial resolution.

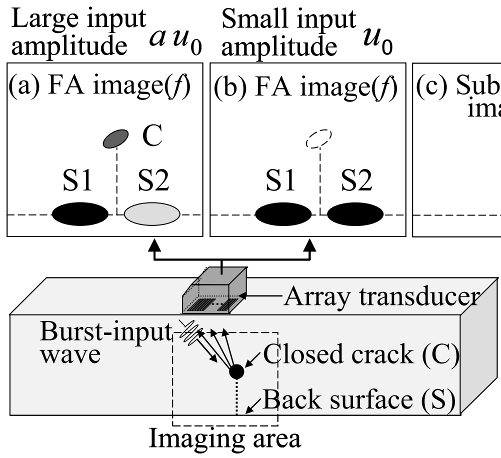


Fig. 1 Principle of the AD method of fundamental waves: (a) Large input amplitude, (b) Small input amplitude multiplied by an amplification factor $a$, (c) Subtracted image ( = (a)-$a$×(b) ).

## 3. Experiment

### 3-1. Experimental condition

Experimental configuration is shown in Fig.

2(a). To verify the AD method of fundamental waves in experiment, a closed fatigue crack specimen[6] was imaged by a single array SPACE.[8] The single array SPACE used a PZT array transducer of 32 elements with a center frequency of 5 MHz for both emission and reception. The focused waves of 3-cycle bursts at a frequency of 7 MHz were excited at 8.9 nm (2.4 MPa) and 26.8 nm (7.3 MPa) as a small and a large input, respectively. The AD of fundamental waves was compared with that of subharmonic waves.

### 3-2. Experimental results

Imaging results of the closed fatigue crack were shown in Figs. 2(b)-2(g). In the SA images [Figs. 2(e) and 2(f)], the closed crack C was imaged at both the large and small input, whereas the ghosts S were also imaged in the back surface and the notch. Therefore, the selectivity was low. Then, the AD method was applied to the SA images. As a result, C was imaged in the subtracted image [Fig. 2(g)], and thereby, the selectivity was enhanced by 7.6 dB. However, S was not completely eliminated. This can be presumed that not only C but also S appears as increment as mentioned in §1.

Here, we employed the wavelet analysis of shift-summation waveform at C at large input, as shown in Fig. 3. We found that not only the subharmonic wave (3.5 MHz) but also the fundamental wave[7] was generated. This would include the fundamental component generated by the contact vibration.

In the FA images [Figs. 2(b) and 2(c)], C was imaged at both the large and small input with higher spatial resolution than that in the SA images, whereas the back surfaces S1 and S2 were also imaged. Therefore, the selectivity was low. Then, the AD method was applied to the FA images. As a result, only C was successfully imaged in the subtracted image [Fig. 2(d)] with canceling S1 and S2, and thereby, the selectivity was dramatically enhanced by 34 dB. Furthermore, the spatial resolution in Fig. 2(d) was higher than in Fig. 2(g). Thus, we verified the advantage of the AD method of fundamental waves over that of subharmonic waves[6].

### 4. Conclusions

We proposed amplitude difference (AD) method utilizing the nonlinearity of fundamental wave due to the contact vibration of closed cracks. We verified that the AD method of fundamental waves can realize the higher selectivity and spatial resolution than that of subharmonic waves. This method would enable us to estimate a closure stress from the input-wave stress at a threshold.

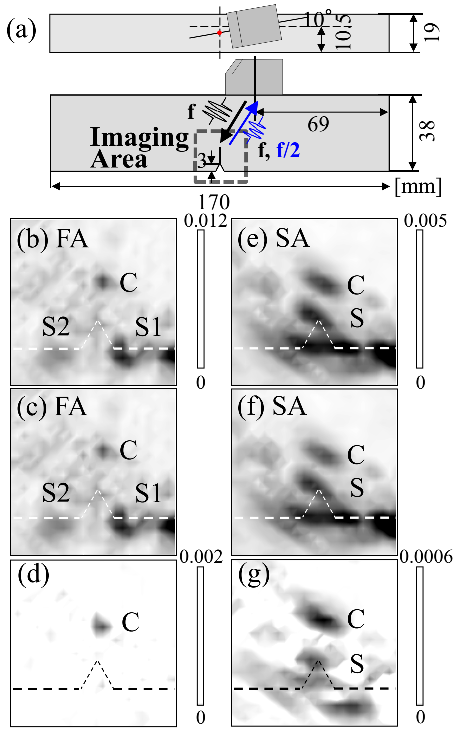


Fig. 2 Experimental configuration and results: (a) Experimental configuration, (b)-(d) FA images at large and small amplitude and their subtracted image. (e)-(g) SA images at large and small amplitude and their subtracted image.

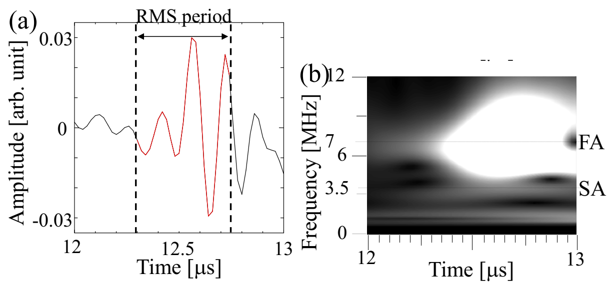


Fig. 3 Shift-summation waveform and frequency analysis at C: (a) Shift-summation waveform. (b) Wavelet analysis.

### Acknowledgments

This work was supported by Grants-in-Aid for Science Research (Nos. 24246119 and 24686081) from the Ministry of Education, Culture, Sports, Science, and Technology of Japan.

### References

1. K. Yamanaka, et al.: JJAP, **43** (2004) 3082.
2. Y. Ohara, et al.: APL, **90** (2007) 011902.
3. H. Arai: Japan Patent 30107 (2002).
4. M. Scalerandi, et al.: APL, **92** (2008) 101912.
5. K. Yamanaka, et al.: APEX, **4** (2011) 076601.
6. Y. Ohara, et al.: JJAP, **51** (2012) 07GB18.
7. Y. Ohara, et al.: Proc. of USE, **27** (2006) 423.
8. Y. Ohara, et al.: Hihakai kensa, **60**(11), (2011) 658. [in Japanese]